THESIS FOR THE DEGREE OF LICENTIATE OF ENGINEERING

Water and hydroxyl in luminous infrared galaxies: Spectroscopic observations and modelling

NIKLAS FALSTAD

CHALMERS

Department of Earth and Space Sciences
CHALMERS UNIVERSITY OF TECHNOLOGY
Göteborg, Sweden 2014

Water and hydroxyl in luminous infrared galaxies: Spectroscopic observations and modelling
NIKLAS FALSTAD

Radio Astronomy & Astrophysics Group
Department of Earth and Space Sciences
Chalmers University of Technology
SE–412 96 Göteborg, Sweden
Phone: +46 (0)31–772 1000

Contact information:
Niklas Falstad
Onsala Space Observatory
Chalmers University of Technology
SE–439 92 Onsala, Sweden

Phone: +46 (0)31–772 5541
Fax: +46 (0)31–772 5590
Email: niklas.falstad@chalmers.se

Printed by Chalmers Reproservice
Chalmers University of Technology
Göteborg, Sweden 2014

Water and hydroxyl in luminous infrared galaxies: Spectroscopic observations and modelling

NIKLAS FALSTAD
Department of Earth and Space Sciences
Chalmers University of Technology

Abstract

Many luminous infrared galaxies (LIRGs) contain compact obscured nuclei (CONs) where luminosities in excess of 10^9 $L_\odot$ emerge from inside dusty regions smaller than 100 pc in diameter. Due to the obscuring material in these regions, the nature of the nuclear power source cannot be determined using direct observations in the optical or IR. In addition, extreme column densities towards the central regions might render these objects heavily Compton-thick, blocking even X-rays originating in the nucleus. It is nevertheless important to reveal and understand the nature of the source behind the high luminosity as this may aid our understanding of the evolution of, and connection between, starbursts and active galactic nuclei (AGN).
This thesis describes the ongoing observational and theoretical work to use far-infrared and submillimeter molecular lines to study the central regions of CONs. From excitation analysis, it is possible to construct models of the molecular lines that probe these regions. These models can then constrain the nature of the buried power source.
Observations of the LIRG Zw 049.057, obtained with the Herschel Space Observatory, are presented. These observations reveal a rich spectrum of highly excited water (H_2O) and hydroxyl (OH), species that couple very well to the intense far-infrared radiation field in the centre of this galaxy. The results of our radiative transfer modelling indicate that Zw 049.057 hosts an optically thick, dusty core with a surface brightness of $10^{13} - 10^{14}$ $L_\odot$ kpc^{-2} and a column density of molecular hydrogen (H_2) approaching 10^{25} cm^{-2}. A surface brightness this high in the central parsecs of a galaxy is expected to arise from a compact starburst or an active galactic nucleus, neither of which can be ruled out based on these results.

Keywords: ISM: molecules – Galaxies: ISM – Galaxies: individual: Zw 049.057 – Line: formation – Infrared: galaxies – Submillimeter: galaxies

Research contributions

This thesis is based on the work contained in **Paper I:**

- N. Falstad, E. González-Alfonso, S. Aalto, P.P. van der Werf, J. Fischer, J. Graciá-Carpio, E. Sturm, S. Veilleux, M. Meléndez, H. W. W. Spoon, H. A. Smith & M. L. N. Ashby :
  Herschel *spectroscopic observations of Zw 049.057*
  Manuscript intended for Astronomy & Astrophysics.

I have also participated in the following papers not included in the thesis:

- E. González-Alfonso, J. Fischer, J. Graciá-Carpio, N. Falstad, E. Sturm, M. Meléndez, H. W. W. Spoon, A. Verma, R. I. Davies, D. Lutz, S. Aalto, E. Polisensky, A. Poglitsch, S. Veilleux & A. Contursi:
  The Mrk 231 molecular outflow as seen in OH
  Astronomy & Astrophysics, 561, A27 (2014)

- E. González-Alfonso, J. Fischer, S. Aalto & N. Falstad:
  Modeling the H_2O submillimeter emission in extragalactic sources
  Astronomy & Astrophysics, 567, A91 (2014)

Acknowledgements

First, I would like to thank my supervisor Susanne Aalto for her help and encouragement during my PhD studies so far. Thank you also to my second supervisor Eduardo González-Alfonso for his patience when teaching me about modelling work. My third supervisor Sebastien Muller and my examiner John Black also deserve a thank you for lending their critical eyes to the drafts of this thesis. A special thank you to my master's thesis supervisor Alessandro Romeo who really led me into astronomy. Thank you also to all my colleagues at the observatory and Chalmers, especially my fellow PhD students, for providing such an inspiring working environment.
Finally, I would like to thank my sister for being there when times have been rough, and Jenni for her love and support while writing this thesis.

Niklas

Contents

Chapter 1

Introduction

Through the analysis of radiation that has travelled to us all the way from the nucleus of another galaxies, we may learn a lot about the conditions in the place where it originated. In order to be able to interpret this radiation we have to construct models of the conditions under which it was formed. That is the topic of this thesis. Based on observations of other galaxies we try to make models of their dusty interiors in an effort to understand what drives them. Unravelling these hidden power sources is of great importance as it will aid our understanding of the evolution of active galactic nuclei (AGN) and starbursts.

It is nevertheless important to reveal and understand the nature of the source behind the high luminosity as this may aid our understanding of the evolution of, and connection between, starbursts and active galactic nuclei (AGN).

This first chapter is devoted to a short introduction to the interstellar medium and a basic description of molecular excitation and radiative transfer. In Chap. 2 we give an account of energetic galaxies and their, sometimes hidden, power sources. Chapter 3 then contains a discussion on how to study the dust-obscured nuclei of these galaxies. Finally, in Chap. 3 we give an introduction to the appended paper.

1.1 The interstellar medium

General references: Tielens (2010); Omont (2007)

Although stars make up a considerable part of the mass of a galaxies, they only fill a very small fraction of the total galactic volume. Filling the void between stellar systems in galaxies is the very tenuous mix of gas and dust referred to as the interstellar medium (ISM). This is the matter from which stars are formed, but the stars themselves also influence the ISM as they inject processed stellar

material and radiative and mechanical energy. This cyclic process drives the chemical evolution of galaxies and studies of the ISM are important to understand their history and to predict their future.

The ISM is a multi-phase medium where ionized, atomic and molecular gas as well as ices and dust particles reside in a variety of different environments. By mass, most of the gas is atomic or molecular hydrogen with lesser amounts of helium and less than one percent of heavier elements. The fraction of heavier elements is however slowly increasing because of the nucleosynthesis that occurs in stars and supernovae. Dust constitutes only ~ 1 % of the total ISM mass but it is an important catalyst for the formation of molecular hydrogen (Hollenbach & Salpeter, 1971) and the major source of opacity for non-ionizing photons. Dust grains are efficient absorbers at ultraviolet (UV) and visual wavelengths, by re-radiating the absorbed light in the infrared the dust can influence the spectral energy distribution of entire galaxies. The grains also lock up a significant fraction of the heavier elements of the ISM and provide a surface for other species to freeze out onto.

1.1.1 Molecules

Molecules play an immensely important role in the ISM as the dense cores of molecular clouds are the sites of star formation. Due to the large domination of hydrogen in the ISM the bulk of the molecular gas is in H_2, with less than 1% of the gas in other molecules. Molecular hydrogen is however hard to observe due to its lack of a permanent dipole moment and the large spacing between its rotational energy levels. Its lowest rotational transition is from the J$= 2$ energy level situated ~ 500 K above the ground state, much higher than the typical temperature of molecular clouds. In order to study the molecular gas we must therefore rely on observations of other molecules.

A common tracer of molecular gas is carbon monoxide (CO), the second most abundant molecular species in the ISM with a typical abundance relative to H_2 of $\sim 10^{-5}-10^{-4}$. It has closely spaced rotational energy levels with the lowest excited level at about 5.5 K and is thus easily excited even in cold environments. An additional advantage is that the three lowest rotational transitions are located at wavelengths where the atmospheric transmission is good, and therefore are observable using ground-based telescopes. However, because of its high abundance the main isotopologue $^{12}C^{16}O$ easily becomes optically thick in its low-lying transitions. This obstacle can be overcome by observing less abundant variants like $^{13}C^{16}O$ or $^{12}C^{18}O$.

CO is tracing gas with moderate density. Molecules like hydrogen cyanide (HCN) and the formyl ion (HCO^+) have higher dipole moments and therefore decay to lower states through radiation faster than CO. Because of this they are not as efficiently excited in the gas probed by CO and the bulk of the emission

will originate in denser gas. This thesis is however focused on absorption and emission of the light hydrides OH and H_2O. These molecules lack important lines in the mm-wavelength domain, but have an abundance of lines in the far-infrared and submillimeter domain. This makes them sensitive to radiative excitation by warm dust emission and they are well suited to probe the physical conditions in the nuclei of dusty galaxies. It also makes their transitions, in sources at low redshift, inaccessible with ground-based telescopes and space-based facilities are therefore needed. H_2O and OH are treated in more detail in Sect. 3.2.

1.1.2 Dust

Although it only contributes a small fraction of its total mass, dust is an important constituent of the ISM. The surfaces of dust grains provide a place for species to accrete and react with each other, thus acting as an important catalyst in the formation of molecules, especially H_2. Accretion onto and desorption from grain surfaces also serve to regulate the gas phase abundances of different species. The most important property of dust in the context of this thesis is however its ability to completely obscure an embedded power source and shift its spectral energy distribution (SED) to far-infrared wavelengths.

The exact composition of dust grains is not well known but the presence of some important constituents has been inferred based on spectral features identified in dust absorption, scattering or emission: a strong feature at 2175 Å is attributed to graphite while broad features at 9.7 and 18 μm indicate the presence of amorphous silicates. If the grain constituents are known the observed wavelength-dependence of dust extinction can be used to derive the size distribution of the dust grains. The most popular one is the so called Mathis-Rumpl-Nordsieck (MRN) distribution first suggested by Mathis et al. (1977). In this model, graphite and silicate grains have a power-law size distribution with $dn/da \propto a^{-3.5}$ where $n(a)$ is the number of particles of size a between 50 and 2500 Å.

1.2 Molecular emission and absorption

General references: Rybicki & Lightman (1979); Tielens (2010); Wilson et al. (2009)

The internal energy of a molecule depends on its electronic, vibrational and rotational energy states. Through transitions between these energy states the molecule can absorb or emit radiation at specific wavelengths that are determined by the energy difference between the involved states. This thesis is focused on the transitions that involve the lowest energies, those between rotational energy states.

1.2.1 Rotational states

In the simplest case, for a rigid diatomic or linear polyatomic molecule in a $^1\Sigma$ electronic state, the rotational energy levels are given by

$$E_{\text{rot}} = hB_{\text{e}}J(J+1), \tag{1.1}$$

where J is the rotational quantum number and B_{e} is the rotational constant defined as

$$B_{\text{e}} = \frac{h}{8\pi^2\Theta_{\text{e}}}, \tag{1.2}$$

where Θ_{e} is the moment of inertia of the molecule. The electric dipole allowed rotational transitions are those with $\Delta J \pm 1$ and for a transition between state J and $J-1$ the energy difference is

$$\Delta E_{\text{rot}} = 2hB_{\text{e}}J. \tag{1.3}$$

Thus, in this simple case, the spectral lines will be equally spaced in frequency. The lowest rotational levels of the linear molecule HCN are shown in Fig. 1.1.

For non-linear molecules the situation is a bit more complicated. An arbitrary molecule can be described by its three principal moments of inertia: Θ_A, Θ_B and Θ_C where the axes are generally chosen so that $\Theta_A \leq \Theta_B \leq \Theta_C$. If all three moments of inertia are equal the molecule is referred to as a spherical top, if two moments of inertia are equal its a symmetric top and if no two moments of inertia are equal the molecule is an asymmetric top. Symmetric tops can be further divided into prolate (cigar-shaped) tops where $\Theta_A < \Theta_B = \Theta_C$ and oblate (disk-shaped) tops where $\Theta_A = \Theta_B < \Theta_C$.

The rotational state of a symmetric top can be described by the rotational quantum number J and its projection onto the axis of symmetry, K. The energy of each state is then given by

$$E_{\text{rot}} = hBJ(J+1) + h(A-B)K^2, \tag{1.4}$$

for a prolate molecule and

$$E_{\text{rot}} = hBJ(J+1) + h(C-B)K^2, \tag{1.5}$$

for an oblate molecule. A, B and C are here the rotational constants given by

$$A = \frac{h}{8\pi^2\Theta_A}, \tag{1.6}$$

$$B = \frac{h}{8\pi^2\Theta_B}, \tag{1.7}$$

$$C = \frac{h}{8\pi^2\Theta_C}. \tag{1.8}$$

Because the energy of a particular state depends on K^2 the sign of K does not matter and all states with $|K| > 0$ are doubly degenerate. The energy level diagram of the prolate symmetric top NH_3 is shown in Fig. 1.1. For symmetric top

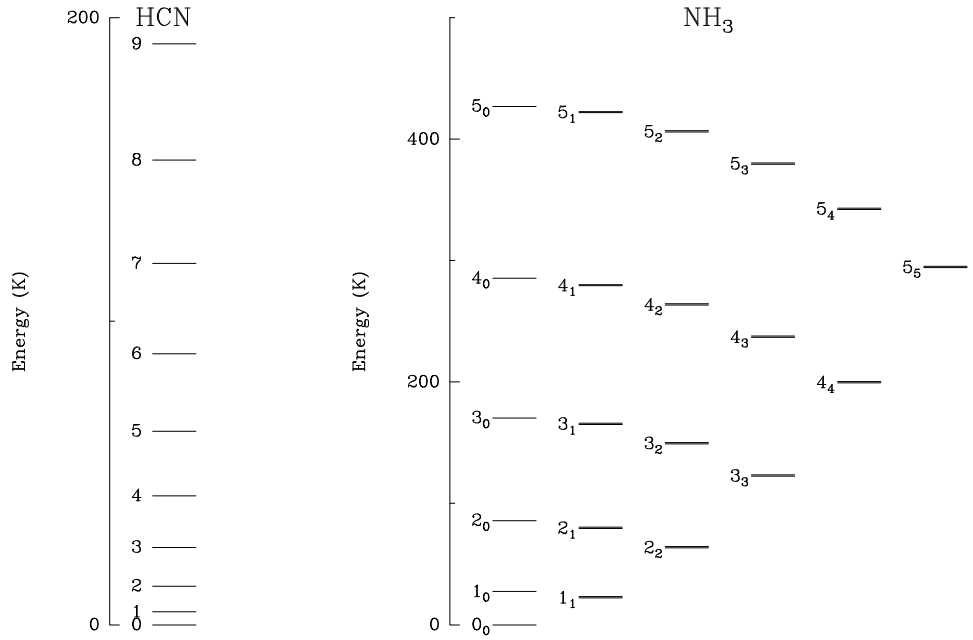

Figure 1.1: Energy level diagrams of the linear molecule HCN and the prolate symmetric top NH_3.

molecules both J and K are time-invariable and thus good quantum numbers. For asymmetric top molecules this is still true for J, but they have no internal molecular axes with a time-invariable component of the angular momentum. One way to describe asymmetric top molecules is to use the rotational quantum number J and the approximate quantum numbers K_a for the limiting prolate top and K_c for the limiting oblate top. In this case there are no simple expressions to describe the energy levels and the deviation from symmetry lifts the degeneracy in energy seen in symmetric top molecules.

1.2.2 Excitation of states

Radiative transitions between the different rotational states occur when the molecule interacts with photons from the surrounding radiation field. A convenient way to treat these transitions is to use the Einstein coefficients. These are A_{ul} which gives the probability for the spontaneous emission of a photon, B_{ul} which gives the probability for the stimulated emission of a photon and B_{lu} which gives the probability for photo absorption. The subscripts u and l refer to the upper and lower energy level, respectively, in each transition. The Einstein coefficients are

related to each other by

$$g_l B_{lu} = g_u B_{ul} \tag{1.9}$$

and

$$A_{ul} = \frac{2h\nu^3}{c^2} B_{ul}, \tag{1.10}$$

where g_l and g_u are the statistical weights of the involved states.

Not only radiative processes affect the molecular excitation and in a proper treatment transitions induced by collisions with other molecules must also be accounted for. The collision rate C_{ij} from level i to level j can be expressed as $C_{ij} = nq_{ij}$ where n is the number density of the collision partner (usually H_2) and q_{ij} is a collisional rate coefficient that depends on the temperature of the gas. When the time scales of chemical processes are sufficiently short, also the state-specific formation and destruction rates, F_i and D_i, must be taken into account (van der Tak et al., 2007).

If the excitation and de-excitation between levels balance in such a way that the level populations do not change with time, the system is said to be in statistical equilibrium (SE). With the Einstein coefficients, collision rates, and state-specific formation and destruction rates in place, we can write down the equations for statistical equilibrium:

$$\begin{aligned} \frac{\mathrm{d}n_i}{\mathrm{d}t} = &\sum_{j<i}^{N} [(n_j B_{ji} - n_i B_{ij}) \bar{J}_{ij} - n_i A_{ij}] \\ &+ \sum_{j>i}^{N} [(n_j B_{ji} - n_i B_{ij}) \bar{J}_{ij} + n_j A_{ji}] \\ &+ \sum_{j\neq i}^{N} [n_j C_{ji} - n_i C_{ij}] + F_i - n_i D_i = 0, \end{aligned} \tag{1.11}$$

where $\bar{J}_{ij}$ is the the intensity of the radiation field averaged over all directions and integrated over the line. In the two simple cases where either black-body radiation or collisions totally dominate the excitation, the relative level populations are given by a Boltzmann distribution with a temperature related to the excitation mechanism at work. When black-body radiation dominates the excitation ($C_{ul} \ll A_{ul}$) the relative populations are given by

$$\frac{n_u}{n_l} = \frac{g_u}{g_l} \exp\left(-\frac{h\nu}{kT_\mathrm{b}}\right), \tag{1.12}$$

where T_b is the temperature of the black-body radiation. If on the other hand collisions dominate the excitation ($C_{ul} \gg A_{ul}$) the relative populations are given

by

$$\frac{n_u}{n_l} = \frac{g_u}{g_l} \exp\left(-\frac{h\nu}{kT_{\rm K}}\right), \tag{1.13}$$

where $T_{\rm K}$ is the temperature that describes the velocity distribution of the colliding particles. In general neither process can be totally neglected and the relative populations are given by

$$\frac{n_u}{n_l} = \frac{g_u}{g_l} \exp\left(-\frac{h\nu}{kT_{\rm ex}}\right), \tag{1.14}$$

where $T_{\rm ex}$ is the temperature needed to correctly describe the excitation of the two levels. Note that in general this excitation temperature is not the same for all transitions.

1.2.3 Radiative transfer

The excitation of molecules discussed in the previous section is dependent on the physical conditions of the surrounding medium. To relate the molecular excitation to these surroundings the transfer of radiation has to be accounted for. Here we will therefore outline the basics of radiative transfer.

A fundamental quantity when dealing with radiative transfer is the specific intensity, I_ν, as this is conserved along a ray through free space. If travelling through a medium it can however change if radiation is absorbed or emitted, this can be described by the equation of transfer

$$\frac{{\rm d}I_\nu}{{\rm d}s} = -\alpha_\nu I_\nu + j_\nu, \tag{1.15}$$

where α_ν is the absorption coefficient and j_ν is the emission coefficient of the medium. For emission and absorption through rotational transitions in molecules the coefficients can be written in terms of the Einstein coefficients and level populations as

$$\alpha_\nu = \frac{h\nu}{4\pi}(n_l B_{lu} - n_u B_{ul})\phi(\nu) \tag{1.16}$$

and

$$j_\nu = \frac{h\nu}{4\pi} n_u A_{ul} \phi(\nu), \tag{1.17}$$

where $\phi(\nu)$ is the line profile. If we now introduce the optical depth

$${\rm d}\tau_\nu = \alpha_\nu {\rm d}s \tag{1.18}$$

and a source function

$$S_\nu = \frac{\jmath_\nu}{\alpha_\nu} = \frac{n_u A_{ul}}{n_l B_{lu} - n_u B_{ul}}, \tag{1.19}$$

the transfer equation (1.15) can be rewritten as

$$\frac{\mathrm{d}I_\nu}{\mathrm{d}\tau_\nu} = -I_\nu + S_\nu. \tag{1.20}$$

Using the integrating factor e^τ we find that the solution to this equation is

$$I_\nu(\tau_\nu) = I_\nu(0)e^{-\tau_\nu} + \int_0^{\tau_\nu} S_\nu(\tau')e^{-(\tau_\nu-\tau')}\mathrm{d}\tau'. \tag{1.21}$$

Assuming a constant source function S_ν this can be further simplified to

$$I_\nu(\tau_\nu) = I_\nu(0)e^{-\tau_\nu} + S_\nu(1-e^{-\tau_\nu}). \tag{1.22}$$

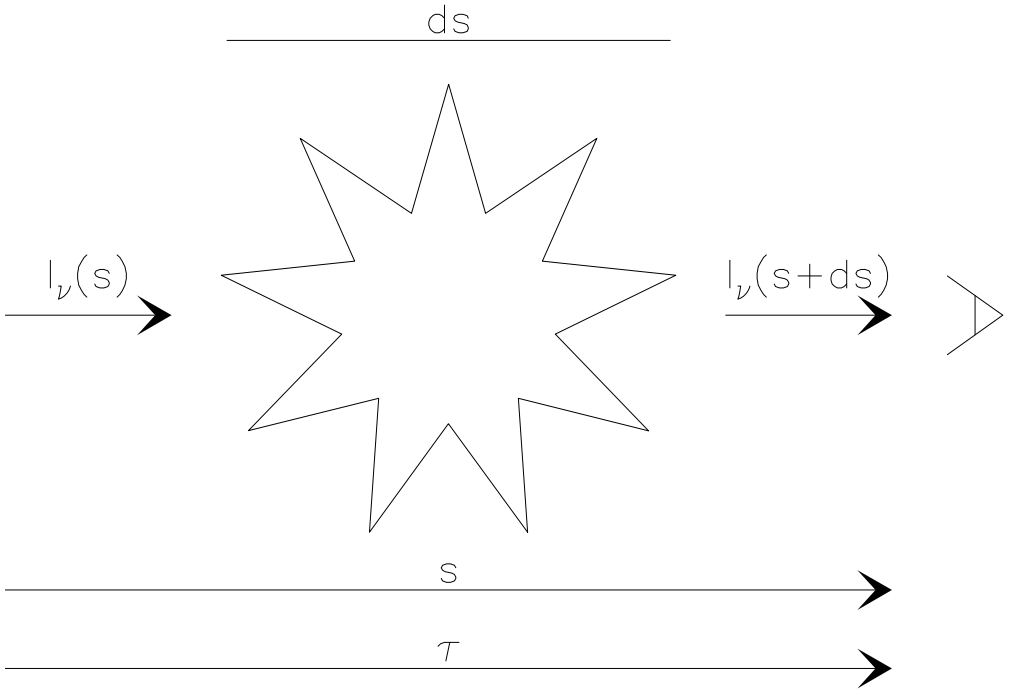

Figure 1.2: Propagation of radiation through a molecular cloud.

An easy interpretation of S_ν in Eq. (1.19) is possible if we rewrite it using the definition of the excitation temperature in Eq. (1.14) together with Eqs. (1.9) and (1.10)

$$S_\nu = \frac{2h\nu^3}{c^2}\frac{1}{\exp\left(\frac{h\nu}{kT_{\mathrm{ex}}}\right)-1}. \tag{1.23}$$

This is just the expression for the radiation field from a black body at temperature T_{ex}. Equation (1.22) for the radiative transfer in a homogeneous medium

can now be written as

$$I_\nu(\tau_\nu) = I_{\nu,\mathrm{bg}} e^{-\tau_\nu} + B_\nu(T_{\mathrm{ex}})(1 - e^{-\tau_\nu}), \tag{1.24}$$

where $I_{\nu,\mathrm{bg}}$ is the intensity of the background radiation.

Now that we have the solution to the transfer equation all we have to do to get the resulting radiation field is to plug in the necessary numbers in Eq. (1.21). Unfortunately both the source function S_ν and the optical depth τ_ν depend on the level populations. To find these we can write down the equations for statistical equilibrium as we did for the two level system in Eq. (1.11). The problem is that we have to know the radiation field in order to solve these equations, the transfer equation and the statistical equilibrium equations are coupled. There are some special cases when this problem disappears, for example in thermal equilibrium when the populations are given by Eq. (1.13), but in general this problem has to be solved by using iterative numerical methods.

Chapter 2

Energetic galaxies

Some galaxies set themselves apart from the rest due to the high luminosities emerging from their centres. Because the total luminosity and spectral energy distribution is generally the result of a combination of different processes, determining the nature of the dominant power source in such galaxies is often complicated. Active galactic nuclei (AGN) and powerful starbursts are both able to dominate the energy output of entire galaxies, these phenomena are discussed In Sects. 2.1 and 2.2, respectively. A group of galaxies where the source of the energy output is not necessarily known is the class of luminous infrared galaxies (LIRGs) discussed in Sect. 2.3. These are classified solely based on the total luminosity at infrared wavelengths and the power source is often hidden behind large columns of dust.

2.1 Active galactic nuclei

General references: Peterson (1997); Courvoisier (2013)

There is no formal definition of AGN, but in general the term is used for energetic phenomena, not directly related to nuclear processes in the interiors of stars, in the central regions of galaxies. It is possible that almost all galaxies contain some kind of active nucleus, but to be recognised as an AGN the activity must contribute a substantial amount of energy over at least some portion of the electromagnetic spectrum. Since the first classification of active nuclei by Seyfert (1943) several subclasses of AGN have been identified. Early discoveries were made independently in the optical and in radio and it was not clear from the start that the objects were of the same underlying nature. A review of the history of AGN from the beginning of the 20th century until the 1980s is given by Shields (1999). A summary of the largest subclasses and their properties can

Table 2.1: Subclasses of AGN

Class	Broad lines	Narrow Lines	Radio loudness
Seyfert 1	Yes	Yes	Radio quiet
Seyfert 2	No	Yes	Radio quiet
Broad line radio galaxies	Yes	Yes	Radio loud
Narrow line radio galaxies	No	Yes	Radio loud
Quasi-stellar objects	Yes	Yes	Radio quiet
Quasars	Yes	Yes	Radio loud
Blazars	No	No	Radio loud

be found in Table 2.1.

The variability on timescales from months down to minutes in some of the objects constrains the size of the emitting region to scales considerably smaller than 1 pc. The extreme luminosities, sometimes outshining entire galaxies, emerging from these tiny regions led to the conclusion that the nature of the power source must be gravitational as nuclear processes are too inefficient. The current understanding is that the origin of the power is accretion of matter onto a supermassive black hole (SMBH). With this in mind, the mass of the compact object can be estimated using the Eddington luminosity, the luminosity above which the radiation pressure from a radiating object powered by spherical accretion exceeds the gravitational attraction of the object. If the radiation pressure is a acting on pure ionized hydrogen the Eddington luminosity is given by

$$L_{\rm Edd} = \frac{4\pi GMc}{\kappa} \simeq 3.2 \times 10^4 \left(\frac{M}{M_\odot}\right) L_\odot, \tag{2.1}$$

where $\kappa = \sigma_{\rm T}/m_{\rm p}$ is the opacity of the ionized gas, $m_{\rm p}$ is the mass of the proton and $\sigma_{\rm T}$ is the Thomson scattering cross-section of the electron. This limit will change if the radiation pressure is mainly acting on material with a different opacity and in a dust enshrouded AGN the effective Eddington limit can be significantly lower (e.g. Fabian et al., 2006). With the brightest observed AGN having luminosities above 10^{13} $\rm L_\odot$ (Türler et al., 1999), the implied mass of the compact object can be as high as 10^9 $\rm M_\odot$. Of course, in order for this to work as a power source, there has to be an ample supply of material close to the nucleus as well as a process in which this material can lose angular momentum and be accreted onto the compact object.

The different subclasses of AGN are very heterogeneous in their observed characteristics but in general they have high luminosities and a relatively flat continuum in νF_ν from X-rays to the far infrared, with a steep decline between 100 μm and radio wavelengths. Other observable characteristics of different types of AGN include the narrow ($\lesssim 1000$ km s^{-1}) permitted and forbidden emission lines of both Type 1 and Type 2 AGN, the broad ($\sim 10,000$ km s^{-1})

permitted emission lines of Type 1 AGN, the radio jets of some radio galaxies, and the rapid variability and high polarization of blazars.

Efforts have been made to explain this observed diversity with a single kind of object observed under different conditions. The most popular such unified models today are those where the apparent diversity arises due to different viewing angles of the object as seen from the Earth (see e.g. Antonucci, 1993; Urry & Padovani, 1995).

2.2 Starburst galaxies

General references: Moorwood (1996)

Some galaxies show signs of recent large-scale star formation activity at a rate significantly higher than in normal galaxies, these are generally referred to as starburst galaxies. The star formation rate (SFR) in these objects is so high, $3 - 30$ $M_\odot$ yr^{-1} in medium luminosity starbursts, that they would consume all the available gas in a short time compared to the life-time of the galaxy. A starburst can therefore clearly be no more than a short phase in the life of a galaxy. Typical characteristics include strong emission-line spectra from HII-regions and a prominent peak in the far infrared associated with emission from dust heated by young massive stars. The vigorous star formation is sometimes located in regions outside the nucleus of the galaxy (e.g. the Antennae Neff & Ulvestad, 2000) but most of the time it is confined to a region in the central kpc, within the context of this thesis we are mainly concerned with these nuclear starbursts.

Although not as compact as AGN, nuclear starbursts also require a process which can transport large amounts of gas into the central regions of the host galaxy to fuel the activity. In order to do this, the gas must lose most of its angular momentum. This can be accomplished by torques created by non-axisymmetric perturbations of the gravitational potential, such as those induced by stellar bars (e.g. Schwarz, 1984; Noguchi, 1988; Shlosman et al., 1989) or interactions with other galaxies (e.g. Mihos & Hernquist, 1996). From IRAS observations Sanders et al. (1986) suggested that the most spectacular starbursts are produced in galaxy mergers. Hybrid N-body/gas dynamics simulations performed by Barnes & Hernquist (1991) showed that the merging of two galaxies can indeed assemble massive amounts of gas in the nucleus of the resulting galaxy.

As for AGN, there are limits to the luminosity of starbursts. In their observations of starbursts around nine Seyfert nuclei Davies et al. (2007) found surface brightnesses approaching 10^{13} $L_\odot$ kpc^{-2} in the central parsecs. As long as the dust temperature is below 200 K these observations can be explained by

an Eddington-like limit based on a model in which the gas disk is supported by stellar radiation pressure (Thompson et al., 2005). Expressed in luminosity per unit mass this limit becomes $500 - 1000$ $L_\odot$ $M_\odot^{-1}$ (Scoville, 2003; Thompson et al., 2005). For higher dust temperatures, the limit to the surface brightness increases two orders of magnitude to 10^{15} $L_\odot$ kpc^{-2} (Andrews & Thompson, 2011).

2.3 Luminous infrared galaxies

General references: Sanders & Mirabel (1996); Lonsdale et al. (2006)

The far-infrared all-sky survey performed with the Infrared Astronomical Satellite (IRAS) in 1983 resulted in the detection of tens of thousands of galaxies, many of which emit most of their energy in the infrared. Although the existence of galaxies with high infrared luminosities was known before IRAS, this was the first time that they where discovered in large numbers and now we know that these infrared galaxies constitute the majority of the most luminous galaxies, those with bolometric luminosities above 10^{11} $L_\odot$, in the local Universe (Sanders & Mirabel, 1996). Two specific classes of galaxies are often mentioned, the luminous infrared galaxies (LIRGs) with luminosities of 10^{11} $L_\odot$ or higher in the $8 - 1000$ μm range and the ultraluminous infrared galaxies (ULIRGs) with luminosities above 10^{12} $L_\odot$ in the same range. Although these constitute the dominant population of objects at high luminosities they are still relatively rare compared to less luminous objects.

The spectral energy distribution (SED) of a typical (U)LIRGs is dominated by a strong starburst-like peak around 60 μm due to warm dust emission, a systematic shift in this peak towards shorter wavelengths can be seen with increasing luminosity. If the galaxy contains an AGN an additional peak can be seen closer to 25 μm due to dust heated directly by the active nucleus. In addition there is a peak in the optical associated with thermal radiation from stars. Note that the optical peak only changes by a factor of about three when the far-infrared emission increase by three orders of magnitude.

The extreme infrared luminosities of (U)LIRGS imply the existence of an energetic power source, heating the large columns of warm dust that is responsible for the bulk of the observed radiation. Due to these large columns of obscuring material the nature of the power source is often unclear, but the large energies involved suggest a compact starburst or an AGN. The most luminous objects all seem to be the results of strong interactions or mergers where copious amounts of gas are funnelled into the nucleus, available to feed a nuclear starburst and/or an AGN. Based on interferometric radio observations Condon et al. (1991) concluded that many of the brightest IRAS galaxies are powered by

nuclear starbursts so compact that they are optically thick to free-free radiation at 1.49 GHz. Due to the Compton-thick nature of such objects, even hard (2-10 keV) X-rays would be unable to penetrate the obscuring material.

Due to the large columns obscuring the nuclei of (U)LIRGs at many wavelengths, alternative probes of the nuclear activity are needed. One widely used diagnostic tool available in some (U)LIRGs are the OH megamasers. These are located in the dense molecular gas in the nuclei of some (U)LIRGs and can have luminosities of a million times those of the strongest Galactic OH masers. The 18 cm lines of OH megamasers can for example be used to detect nuclear outflows in otherwise obscured galaxies (Baan et al., 1989). Later in this thesis we will investigate the ability of H_2O and OH to probe deeper into the far-infrared radiation field to learn more about the physical conditions in obscured nuclei.

2.3.1 Compact obscured nuclei

In some LIRGs the bulk of the activity is confined to their compact obscured nuclei (CONs) where bolometric luminosities larger than 10^9 $L_\odot$ emerge from regions less than 100 pc in diameter with large columns ($N(H_2) > 10^{24}$ cm^{-2}) of warm ($T > 100$ K) molecular gas. The intense IR fields and shielded environments in these objects give rise to rich molecular excitation. A good example is the central region of the LIRG NGC 4418 where vibrational temperatures of 200-400 K in HCN, HNC and HC_3N are found within a core of radius less than 5 pc (Aalto et al., 2007; Costagliola & Aalto, 2010; Sakamoto et al., 2010; Costagliola et al., 2013). Other CONs with hot and optically thick dust cores which have been identified in the near Universe include: Arp 220 (Sakamoto et al., 2008), NGC 1377 (Aalto et al., 2012), IC 860 and Zw 049.057 (Paper I).

The molecular gas rotating in the cores of these compact regions both feeds and obscures the nuclear activity responsible for the high energies involved. As the activity in these objects might be very young, the physical conditions and kinematics of the molecular ISM could therefore provide important clues about the initial stages of nuclear activity in galaxies. Unfortunately the obscuring material of the CONs may be opaque at most wavelengths, effectively hiding the central regions from examination using conventional methods like optical and IR lines and maybe even X-rays. It is therefore important to find tracers that are able to penetrate the optically thick barrier and convey information about the extreme environment close to the nucleus. This can be accomplished by molecular species that are radiatively excited by the intense infrared field near the nucleus and then emit at longer wavelengths where the optical depth is lower. For example, rotational lines of vibrationally excited molecules like HCN, HNC and HC_3N can be used to probe deep into the cores of CONs (Aalto, 2013). Another example are the light hydrides H_2O and OH which couple very well to the far-infrared field, we will discuss them further in Sect. 3.2.

Chapter 3

Conditions in the nuclei of luminous infrared galaxies

As noted in the previous chapter, studies of the compact nuclei in some (U)LIRGs are important for our understanding of the onset and evolution of nuclear activity in galaxies. A short review of recent attempts to do this using radiative transfer codes to model the far-infrared and submillimeter spectra of light hydrides like H_2O and OH is given in this chapter. In Sect. 3.1 the basic conditions for observations of far-infrared and submillimeter radiation are summarized followed by a short description of the Herschel Space Observatory. Section 3.2 then focuses on H_2O and OH and why they are such excellent probes of the intense infrared radiation field in CONs. Finally, Sect. 3.3 contains a summary of observations and radiative transfer modelling of CONs in the local Universe.

3.1 Observations in the far infrared and submillimeter

The emission from rotational transitions in molecules generally occur at wavelengths ranging from the radio for heavy polyatomic species to the far-infrared for light hydrides like H_2O. Due to atmospheric absorption not all of these wavelength regions are available to telescopes located on the ground. For radio waves this is not a big problem, but a lot of the radiation at shorter wavelengths, especially those corresponding to the absorption bands of abundant species like O_2 and H_2O, is absorbed. At submillimeter wavelengths ground-based observations are still possible in certain atmospheric windows, but they generally require high and dry sites to minimize absorption by atmospheric water vapour. This is the reason for the location of, for example, the Atacama Large Millimeter/submillimeter Array (ALMA) at the Chajnantor plateau in the Atacama desert of Chile. At frequencies above ~ 1 THz (wavelengths below

~ 300 μm) most of the radiation is however absorbed by atmospheric species even at these sites. In order to do observations at these wavelengths one alternative is to use airborne observatories like the Stratospheric Observatory for Infrared Astronomy (SOFIA). To avoid the problem with absorption in the atmosphere altogether, space-based observatories like ISO and Herschel have been employed for observations from infrared to submillimeter wavelengths.

3.1.1 Herschel Space Observatory

The Herschel Space Observatory was a space-based observatory in the $55 - 671$ μm spectral range operating from 2009 until 2013 when it ran out of liquid helium used for cooling its instruments. With its 3.5 m Cassegrain antenna it is still the largest space telescope ever launched. Herschel was put in an orbit around the second Lagrangian point (L2) of the Earth-Sun system, where the gravitational forces from the Earth and the Sun makes it possible for an object to orbit the Sun with the same period as the Earth. Onboard, it carried three instruments: the Photodetector Array Camera and Spectrometer (PACS), an imaging photometer and spectrometer covering the spectral range $55 - 210$ μm; the Spectral and Photometric Imaging Receiver (SPIRE), an imaging photometer and spectrometer covering the spectral range $194 - 672$ μm; and the Heterodyne Instrument for the Far Infrared (HIFI), a heterodyne spectrometer covering the frequencies $480 - 1250$ GHz and $1410 - 1910$ GHz.

3.2 H_2O and OH as probes of the warm dust emission in CONs

In order to study the dusty cores of CONs we need a probe that is sensitive to the intense far-infrared radiation fields present in these objects. Due to their small moments of inertia the light hydrides have large rotational constants and thus large differences in energy between their rotational levels, see Sect. 1.2.1 for the equations governing the energies of rotational levels in molecules. Because of this, a large number of their transitions occur at far-infrared or submillimeter wavelengths.

The asymmetric top molecule H_2O has a multitude of rotational transitions at the wavelengths of interest, its rich spectrum spans the entire far-infrared and submillimeter portions of the electromagnetic spectrum available to PACS and SPIRE. Due to its relatively high dipole moment, the transitions of H_2O have fast radiative rates and as long it is not located in an extremely warm and dense environment H_2O is an excellent probe of the underlying far-infrared continuum. With the exception of the ground-state $1_{11} \rightarrow 0_{00}$ transition, the lines with rest wavelengths in the SPIRE spectral range are almost always seen in emission. Modelling of these lines performed by González-Alfonso et al. (2014) suggests that they are pumped by the far-infrared continuum where four absorp-

tion lines at approximately 45, 58, 75, and 101 μm can account for the emission. For the $1_{11} \rightarrow 0_{00}$ line there exists no such pumping mechanism and the upper level can only be radiatively excited by a photon with the same frequency as the line emission. This line is therefore more sensitive to collisional excitation and thus to the density and temperature of the surrounding gas. In the right part of Fig. 3.1 the energy level diagram of H_2O is displayed with lines indicating the transitions that where detected with PACS and SPIRE in Paper I.

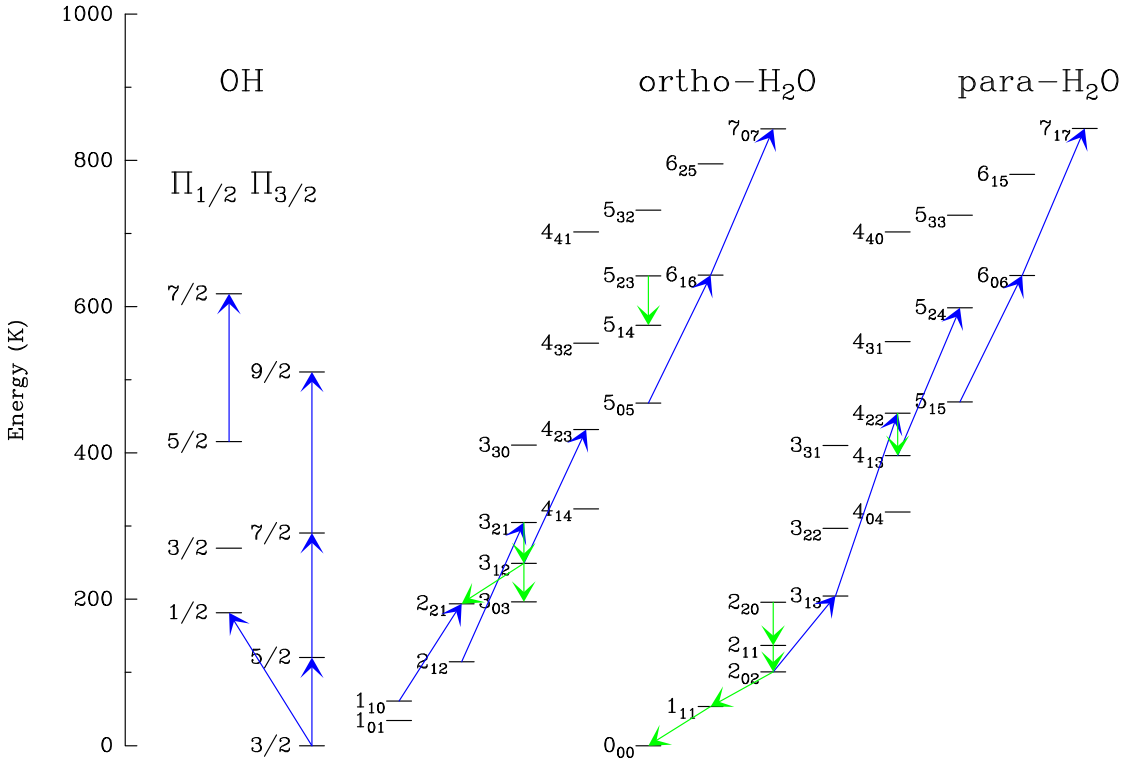

Figure 3.1: Energy level diagrams of OH and H_2O (ortho and para). Blue arrows indicate lines observed with PACS and green arrows denote lines observed with SPIRE.

Like H_2O, OH also has a relatively high dipole moment and many transitions in the far infrared. Unlike H_2O, OH has non-zero electronic angular momentum in the ground state which interacts with the rotation of the molecule to create energy-level splitting in the rotational levels, so-called Λ-doubling. Because of this the far-infrared lines of OH come in the form of doublets as seen in Fig. 3.2. In regions with a strong far-infrared radiation field the levels are expected to be radiatively excited, but the ground state lines, specially the $\Pi_{3/2} - \Pi_{3/2}\, \frac{5}{2} - \frac{3}{2}$ transition at approximately 119 μm, can still be affected by collisional excitation. In the left part of Fig. 3.1 the energy level diagram of OH is displayed with lines indicating the transitions that where detected with PACS in Paper I. OH has also proven to be a good tracer of massive molecular

outflows (Fischer et al., 2010; Sturm et al., 2011).

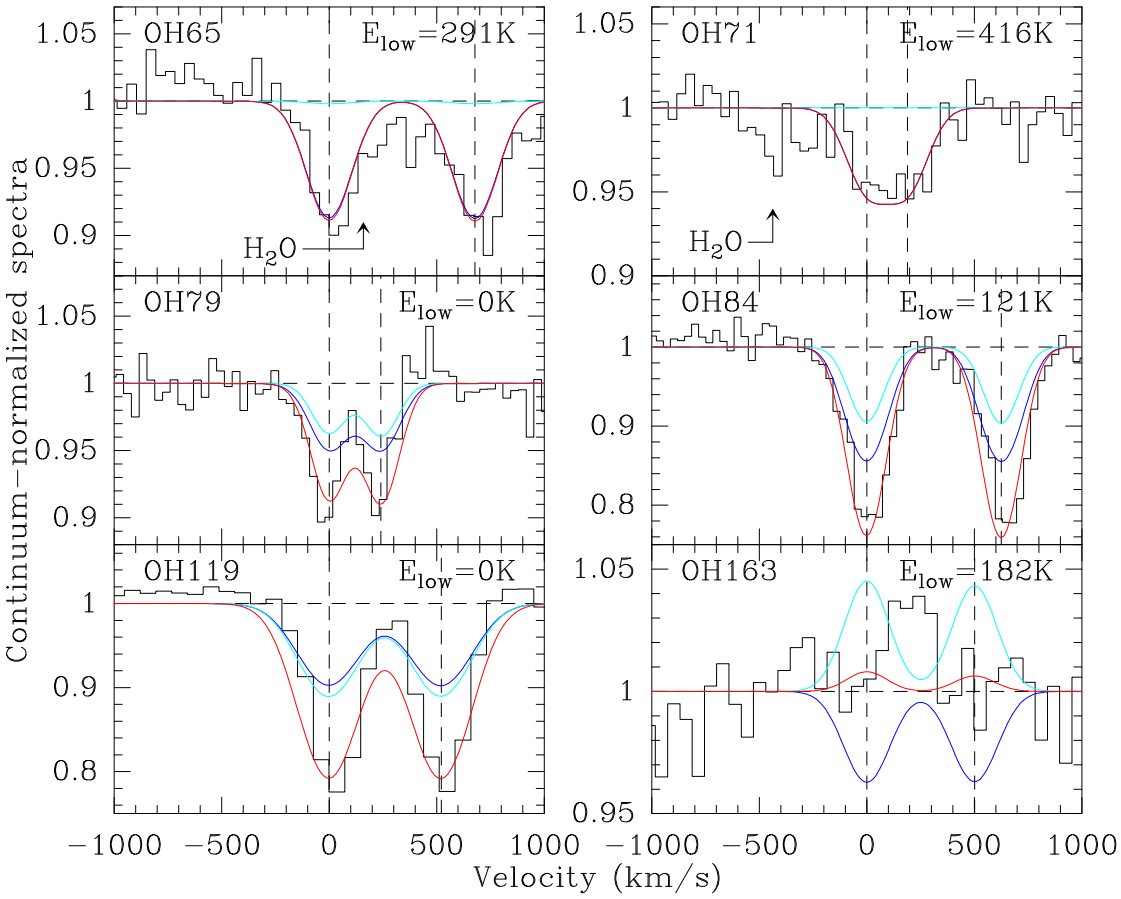

Figure 3.2: Far-infrared OH doublets observed in Zw 049.057 with PACS, the coloured lines represent models from Paper I.

3.3 Radiative transfer models

With their multiple transitions in the far infrared, H_2O and OH are excellent probes of warm dust in the nuclear regions of LIRGs. Observations and subsequent radiative transfer modelling of these species together with the dust continuum make is possible to put constraints on important properties such as the temperature and optical depth of the dust. We will here give a short summary of previous modelling work based on first ISO and then Herschel observations. While H_2O and OH are the main species concerned in this thesis, many of the following authors have also used other species in their analyses.

When ISO opened up the mid- and far-infrared wavelength regimes for spec-

troscopy it became possible to study the dusty nuclei of LIRGs in detail. Based on observations with ISO, Spinoglio et al. (2005) were able to model the overall continuum as well as the atomic spectrum of NGC 1068 with a combination of an AGN and a starburst. In addition, they performed an analysis of the OH lines at 79, 119, and 163 μm which were all detected in emission in this source. They concluded that, unlike the lines at 79 and 163 μm, the OH line at 119 μm cannot be radiatively excited in NGC 1068 but must originate in a region of warm and dense gas where it is collisionally excited. The results of their radiative transfer model further led them to conclude that the bulk of the OH emission arises in the nuclear region of the galaxy, possibly with small contributions from the extended starburst.

Models of the ULIRGs Arp 220 and Mrk 231 by González-Alfonso et al. (2004) and González-Alfonso et al. (2008), respectively, revealed warm, optically thick nuclear regions with dust temperatures of ~ 100 K within diameters of ~ 100 pc. In both sources the excitation of H_2O and OH could be explained by radiative excitation by the far-infrared emission from this warm dust. While both galaxies were found to have high column densities of H_2O and OH towards their nuclei, the models of Arp 220 indicated an H_2 column of $\sim 10^{25}$ cm^{-2}, high enough to obscure a buried X-ray source.

The limits to the spectral resolution and sensitivity of ISO put some constraints on the ability to detect weaker lines and determine the kinematics associated with e.g. the OH detections. With the advent of Herschel it became possible to make observations with higher resolution and sensitivity.

With these new observations at hand, Fischer et al. (2010) detected a molecular outflow in OH and ^{18}OH with velocities in excess of 1000 km s^{-1} in Mrk 231. Besides the high outflow velocities, modelling of the emission indicated an extremely low ^{16}O/^{18}O ratio of $\sim 30 - 40$ which they suggested may be due to advanced starburst activity. In the SPIRE spectrum of the same galaxy, González-Alfonso et al. (2010) detected seven rotational lines of H_2O with upper level energies as high as 640 K. Their radiative transfer models indicated the presence of a warm (~ 100 K) dust component with a radius of ~ 100 pc that is able to radiatively excite the high-lying lines through absorption of far-infrared photons. In addition they noted that a cooler component with a radius of ~ 600 pc is needed to fully account for the lower-lying lines. They conclude that although it gave new clues to the origin of H_2O in Mrk 231, their new analysis supports their old conclusions that where based on observations with ISO.

Based on full range PACS spectroscopy González-Alfonso et al. (2012) performed an analysis of the excitation in Arp 220 and the LIRG NGC 4418. They found very high excitation in H_2O, OH, HCN and NH_3 in both galaxies but overall the excitation was somewhat higher in NGC 4418 than in Arp 220. To account for this high excitation, the radiative transfer models indicated the need for warm (> 100 K), optically thick dust components in the nuclei of both galax-

ies. These nuclear components both have high surface brightnesses in excess of 10^{13} $L_\odot$ kpc^{-2} which the authors suggest are due to either deeply buried AGN or hyper star clusters. This is also consistent with the high column densities of H_2, higher than 10^{25} cm^{-2}, which they find towards the cores of both galaxies. In Arp 220 they detect an outflow while in NGC 4418 there is an apparent inflow onto the nucleus. A strong enhancement of ^{18}O with a ^{16}O/^{18}O ratio of $70 - 130$ is inferred in Arp 220 while NGC 4418 seems to have a ratio similar to the solar system isotopic ratio. The authors suggest that the differences in kinematics and ^{18}O enhancement in the two galaxies are due to different evolutionary stages where the activity in Arp 220 is in a later stage and both galaxies are in an earlier phase than Mrk 231.

Chapter 4

Introduction to paper I

The LIRG Zw 049.057 is an edge-on early type disk galaxy with a compact radio core and an OH megamaser. It exhibits deep mid-infrared silicate absorption and a rich molecular spectrum. This paper is based on observations of Zw 049.057 taken with PACS as part of the Herschel OT2 programme Hermolirg (PI: E. González-Alfonso) and with SPIRE as part of the OT key programme Hercules (PI: P.P. van der Werf). These observations revealed emission and absorption of highly excited H_2O as well as absorption of both OH and ^{18}OH. Although not reported in this paper, absorptions of other light hydrides as well as many lines from molecular ions were also detected. In this paper we have used the radiative transfer code described in González-Alfonso & Cernicharo (1999) to analyse these rich spectra and construct a model of the nuclear components of Zw 049.057.

We find that a minimum of two components are needed to account for the absorption lines of H_2O and OH in this galaxy. The high excitation lines require a compact, nuclear component with warm ($100 - 120$ K) dust and high abundances of both H_2O and OH. The estimated column density of H_2 towards this component may be as high as 10^{25} cm^{-2} and a buried X-ray source would be difficult to detect even in hard X-rays. In addition, the surface brightness of the component is between 10^{13} and 10^{14} L$_\odot$ kpc^{-2}, indicative of either a buried AGN or a very dense nuclear starburst. The ^{16}O/^{18}O ratio of $75 - 150$ required to reproduce the ^{18}OH absorptions would place Zw 049.057 close to Arp 220 in the evolutionary scheme tentatively suggested by González-Alfonso et al. (2012) for NGC 4418, Arp 220, and Mrk 231. To also reproduce the emission lines in the submillimeter, an additional cooler ($40 - 50$ K) and less dense component is required.

4.1 Future prospects

The Herschel observations also revealed emission and absorption of other light hydrides as well as many lines from molecular ions. Modelling of the molecular ions could e.g. provide important information about the oxygen chemistry in the ISM of Zw 049.057. Some of the absorption lines reported in paper I exhibit tentative in- and outflow signatures which we did not attempt to model. Further study of these features would provide information about the gas motions they are possibly tracing. We are also in possession of interferometric mm-data which can help our understanding on the spatial structure of Zw 049.057.

Bibliography

Aalto, S. 2013, in IAU Symposium, Vol. 292, IAU Symposium, ed. T. Wong & J. Ott, 199–208

Aalto, S., Monje, R., & Martín, S. 2007, A&A, 475, 479

Aalto, S., Muller, S., Sakamoto, K., et al. 2012, A&A, 546, A68

Andrews, B. H. & Thompson, T. A. 2011, ApJ, 727, 97

Antonucci, R. 1993, ARA&A, 31, 473

Baan, W. A., Haschick, A. D., & Henkel, C. 1989, ApJ, 346, 680

Barnes, J. E. & Hernquist, L. E. 1991, ApJ, 370, L65

Condon, J. J., Huang, Z.-P., Yin, Q. F., & Thuan, T. X. 1991, ApJ, 378, 65

Costagliola, F. & Aalto, S. 2010, A&A, 515, A71

Costagliola, F., Aalto, S., Sakamoto, K., et al. 2013, A&A, 556, A66

Courvoisier, T. J.-L. 2013, High Energy Astrophysics

Davies, R. I., Müller Sánchez, F., Genzel, R., et al. 2007, ApJ, 671, 1388

Fabian, A. C., Celotti, A., & Erlund, M. C. 2006, MNRAS, 373, L16

Fischer, J., Sturm, E., González-Alfonso, E., et al. 2010, A&A, 518, L41

González-Alfonso, E. & Cernicharo, J. 1999, ApJ, 525, 845

González-Alfonso, E., Fischer, J., Aalto, S., & Falstad, N. 2014, A&A, 567, A91

González-Alfonso, E., Fischer, J., Graciá-Carpio, J., et al. 2012, A&A, 541, A4

González-Alfonso, E., Fischer, J., Isaak, K., et al. 2010, A&A, 518, L43

González-Alfonso, E., Smith, H. A., Ashby, M. L. N., et al. 2008, ApJ, 675, 303

González-Alfonso, E., Smith, H. A., Fischer, J., & Cernicharo, J. 2004, ApJ, 613, 247

Hollenbach, D. & Salpeter, E. E. 1971, ApJ, 163, 155

Lonsdale, C. J., Farrah, D., & Smith, H. E. 2006, Ultraluminous Infrared Galaxies, ed. J. W. Mason, 285

Mathis, J. S., Rumpl, W., & Nordsieck, K. H. 1977, ApJ, 217, 425

Mihos, J. C. & Hernquist, L. 1996, ApJ, 464, 641

Moorwood, A. F. M. 1996, Space Sci. Rev., 77, 303

Neff, S. G. & Ulvestad, J. S. 2000, AJ, 120, 670

Noguchi, M. 1988, A&A, 203, 259

Omont, A. 2007, Reports on Progress in Physics, 70, 1099

Peterson, B. M. 1997, An Introduction to Active Galactic Nuclei

Rybicki, G. B. & Lightman, A. P. 1979, Radiative processes in astrophysics

Sakamoto, K., Aalto, S., Evans, A. S., Wiedner, M. C., & Wilner, D. J. 2010, ApJ, 725, L228

Sakamoto, K., Wang, J., Wiedner, M. C., et al. 2008, ApJ, 684, 957

Sanders, D. B. & Mirabel, I. F. 1996, ARA&A, 34, 749

Sanders, D. B., Scoville, N. Z., Young, J. S., et al. 1986, ApJ, 305, L45

Schwarz, M. P. 1984, MNRAS, 209, 93

Scoville, N. 2003, Journal of Korean Astronomical Society, 36, 167

Seyfert, C. K. 1943, ApJ, 97, 28

Shields, G. A. 1999, PASP, 111, 661

Shlosman, I., Frank, J., & Begelman, M. C. 1989, Nature, 338, 45

Spinoglio, L., Malkan, M. A., Smith, H. A., González-Alfonso, E., & Fischer, J. 2005, ApJ, 623, 123

Sturm, E., González-Alfonso, E., Veilleux, S., et al. 2011, ApJ, 733, L16

Thompson, T. A., Quataert, E., & Murray, N. 2005, ApJ, 630, 167

Tielens, A. G. G. M. 2010, The Physics and Chemistry of the Interstellar Medium

Türler, M., Paltani, S., Courvoisier, T. J.-L., et al. 1999, A&AS, 134, 89

Urry, C. M. & Padovani, P. 1995, PASP, 107, 803

van der Tak, F. F. S., Black, J. H., Schöier, F. L., Jansen, D. J., & van Dishoeck, E. F. 2007, A&A, 468, 627

Wilson, T. L., Rohlfs, K., & Hüttemeister, S. 2009, Tools of Radio Astronomy (Springer-Verlag)